In Situ Blood–Brain Barrier Transport of Nanoparticles

Joanna M. Koziara,[1] Paul R. Lockman,[2] David D. Allen,[2] and Russell J. Mumper[1,3]

Received March 26, 2003; accepted July 2, 2003

Purpose. Two novel types of nanoparticles were evaluated as potential carriers for drugs across the blood–brain barrier (BBB).

Methods. Nanoparticles were composed of biocompatible materials including emulsifying wax (E. Wax) or Brij 72. Brij 78 and Tween 80 were used as surfactants for E.Wax nanoparticles (E78 NPs) and Brij 72 nanoparticles (E72 NPs), respectively. Both nanoparticle formulations were prepared from warm microemulsion precursors using melted E. Wax or Brij 72 as the oil phase. Nanoparticles were radiolabeled by entrapment of [^{3}H]cetyl alcohol, and entrapment efficiency and release of radiolabel were evaluated. The transport of E78 and E72 NPs across the BBB was measured by an *in situ* rat brain perfusion method.

Results. Both formulations were successfully radiolabeled by entrapment of [^{3}H]cetyl alcohol; ~98% of radiolabel remained associated with nanoparticles at experimental conditions. The transfer rate (K_{in}) of E78 NPs from perfusion fluid into the brain was $4.1 \pm 0.5 \times 10^{-3}$ ml/s/g, and the permeability–surface area product (PA) was $4.3 \pm 0.7 \times 10^{-3}$ ml/s/g. The values for K_{in} and PA for E72 NPs were $5.7 \pm 1.1 \times 10^{-3}$ ml/s/g and $6.1 \pm 1.4 \times 10^{-3}$ ml/s/g, respectively.

Conclusions. For both nanoparticle types, statistically significant uptake was observed compared to [^{14}C]sucrose, suggesting central nervous system uptake of nanoparticles. The mechanism underlying the nanoparticle brain uptake has yet to be fully understood.

KEY WORDS: brain perfusion; microemulsion; polysorbate 80; emulsifying wax; Brij.

INTRODUCTION

The entry of drug molecules into the brain is limited by one of the strictest barriers: the blood–brain barrier (BBB). The BBB consists of a continuous layer of endothelial cells joined together by tight junctions (zonulae occludens), which severely restrict paracellular transport across the barrier (1). The BBB allows for passive diffusion of small lipid-soluble molecules, whereas hydrophilic substances or molecules with high molecular weight have minimal passive permeation. Transport across the BBB is additionally regulated by a number of transporters including very effective efflux transporters such as multidrug resistance-associated protein (MRP) or p-glycoprotein (pgp) (2).

There have been a number of attempts to overcome this tight endothelial barrier in order to deliver drugs for various central nervous system (CNS) disorders. One of the strategies involves artificially opening the BBB by administration of hyperosmotic agents or vasoactive molecules, e.g., bradykinin, histamine, serotonin (1). Although compromising BBB integrity allows for paracellular transport of polar drug molecules into the brain, there is potential danger of toxicity caused by CNS entry of other unwanted molecules. Other methods to circumvent the BBB have also been intensively explored. These include intracerebroventricular injections or implantation of polymeric devices directly into the brain (1,3,4). Diffusion of drug molecules, such as proteins, is limited in the brain tissue. Thus, delivery systems must be implanted in close proximity to targeted cells without disruption of neighboring neurons. Although some studies show potential benefits, the necessity of neuroinvasive surgery limits these methods. Intranasal administration has been proven to allow for uptake of some molecules into the brain. The olfactory nerve pathway allows bypassing the BBB; however, uptake by olfactory neurons depends on lipophilicity and molecular weight of the drug. If the drug molecule is transported to the CNS by the olfactory epithelial pathway, it reaches cerebrospinal fluid (CSF) and therefore must cross the functional CSF-brain barrier (5,6). An alternative strategy to overcome the BBB is the use of drug carrier systems such as liposomes (1,2), antibodies (7), or solid nanoparticles (8,10).

Solid nanoparticles are small (1–1000 nm) colloidal particles in which a drug can be entrapped or embedded in the nanoparticle matrix or adsorbed on their surface. Nanoparticles have been shown to effectively deliver drugs in a controlled manner (9). Numerous studies have been performed to demonstrate the potential use of nanoparticles as drug carriers for brain targeting (8,10–15). Poly(butylcyanoacrylate) (PBCA) nanoparticles coated with polysorbate 80 have been shown to successfully deliver drugs *in vivo* to the CNS (10). The hexapeptide dalargin, a Leu-enkephalin analogue with no BBB permeability, adsorbed to the surface of PBCA nanoparticles caused central analgesia in mice after intravenous administration (12,16). Other drugs such as tubocurarine (11), doxorubicin (13), kytorphin (14), and loperamide (15) were successfully delivered to the animal brain *in vivo.* Brain uptake of nanoparticles in these studies was suggested based on the fact that drugs adsorbed to PBCA nanoparticles caused a resultant pharmacologic effect in the CNS (11,12,14). The brain distribution of drugs delivered on the surface of nanoparticles was also confirmed by quantification of the drug itself in brain tissue (13,17). Studies have also demonstrated uptake of intact nanoparticles *in vivo.* Troster *et al.* investigated biodistribution of [^{14}C]poly(methylmethacrylate) nanoparticles coated with various surfactants in rats. These authors observed up to a 13-fold increase of radioactivity in the brain with surfactant-coated nanoparticles over uncoated nanoparticles (18). Kreuter and colleagues performed fluorescent and electron microscopy studies to investigate the possibility of endothelial cell uptake of PBCA nanoparticles (19). PBCA nanoparticles labeled with fluorescein isothiocyanate dextran were administered intravenously to mice. Animals were sacrificed, and brain tissue was analyzed for nanoparticle presence. Fluorescence was observed acentrally in brain blood vessels and in Purkinje cells of the cerebellum, suggesting interaction of polysorbate 80–coated nanoparticles with the endothelium and subsequent transport across the BBB. However, this study was conducted on two animals, and no quantification analysis was performed (19).

[1] Division of Pharmaceutical Sciences, College of Pharmacy, University of Kentucky, Lexington, KY 40536-0082.

[2] Department of Pharmaceutical Sciences, School of Pharmacy, Texas Tech University Health Sciences Center, Amarillo, Texas 79106-1712.

[3] To whom correspondence should be addressed. (email: rjmump2@email.uky.edu)

0724-8741/03/1100-1772/0 © 2003 Plenum Publishing Corporation

The objective of this present study was to assess the brain uptake of two novel nanoparticle-based systems. Emulsifying wax nanoparticles (E78 NPs) made with Brij 78 as the surfactant and Brij 72 nanoparticles (E72 NPs) made with Tween 80 as the surfactant were engineered from microemulsion precursors. Nanoparticles were radiolabeled, and their transport across the BBB was quantified *in vivo* using a rat brain perfusion method.

MATERIALS AND METHODS

Emulsifying wax (E. Wax), polyoxyethylene 20-sorbitan monooleate (Tween 80, polysorbate 80), polyoxyl 2-stearyl ether (Brij 72), and DispoDialyzers MWCO 100 kDa were purchased from Spectrum Chemicals (New Brunswick, NJ). Polyoxyl 20-stearyl ether (Brij 78) was obtained from Uniquema (Wilmington, DE). Sephadex G-75, phosphate-buffered saline (PBS), and sodium chloride were purchased from Sigma Chemicals (St. Louis, MO). 1-[^{3}H]hexadecanol (1 mCi/ml; radiochemical purity greater than 96%) was purchased from Moravek Biochemicals (Brea, CA), and [^{14}C]sucrose (4.75 mCi/mmol) was obtained from Dupont-New England Nuclear (Boston, MA). Materials were used as obtained. For all experiments deionized water was filtered through 0.2-μm filters (Nalgene International, Rochester, NY).

Preparation of Nanoparticles from Microemulsion Precursors

Microemulsion precursors were prepared as reported by Oyewumi and Mumper (20). Briefly, 2 mg of E. Wax or Brij 72 was weighed out into glass vials. Deionized, 0.2-μm filtered water was added, and the mixture was heated to 50–55°C under stirring conditions to melt the E. Wax or Brij 72. To the milky slurry of E. Wax in water, an aliquot of 100 mM Brij 78 was added to obtain a final volume of 1 ml and final surfactant concentration of 3 mM. Microemulsions formed spontaneously after the addition of surfactant. Warm microemulsion precursors formed solid E78 NPs upon simple cooling to room temperature under stirring conditions. Brij 72 nanoparticles were prepared by the same method with 2.3 mM Tween 80 as final surfactant concentration. The final concentration of nanoparticles in all samples was 2 mg/ml.

Characterization of Nanoparticles

Particle size was measured at 20°C using a Coulter N4 Plus Sub-Micron Particle Sizer (Coulter Corporation, Miami, FL) at 90-degree light scattering for 90 s. Before size determination, nanoparticle suspensions were diluted with filtered water to ensure light scattering intensities within the required range of the instrument (5×10^4 to 1×10^6 counts/s).

The stability of nanoparticles was assessed over time based on retention of particle size and was determined at various temperatures (–20°C, 4°C, 25°C, and 37°C) and in several different media: 10 mM PBS pH 7.4, 150 mM sodium chloride, 10% (v/v) fetal bovine serum in 150 mM NaCl, and water. Nanoparticle suspensions were sealed and stored at the tested temperatures. Before dilution for particle sizing, samples were left to equilibrate to room temperature. The stability of nanoparticle formulations was also determined in various media at physiologic (37°C) and room temperatures by dilution of the nanoparticles 1:10 v/v.

Nanoparticle Radiolabeling

Nanoparticles were radiolabeled by entrapment of [^{3}H]hexadecanol (cetyl alcohol). Radioactive cetyl alcohol in methanol was pipetted into glass vials containing E. Wax or Brij 72. Vials were left on a hot plate (50°C) to allow complete evaporation of methanol. After evaporation of methanol, nanoparticles were formulated as described in above. All preparations were formulated with theoretical activities of 150 μCi per ml of final preparation.

Characterization of Radiolabeled Nanoparticles ([^{3}H]NPs)

The entrapment efficiency of [^{3}H]cetyl alcohol was determined using gel permeation chromatography (GPC). To obtain GPC elution profiles, 200 μl of radioactive nanoparticle suspension was eluted through Sephadex G-75 columns (150 × 70 mm) with 10 mM PBS as the mobile phase. Nanoparticles were detected by light scattering counts per second (CPS) and liquid scintillation counting (LSC). Additionally, a control sample of 300 μl of water spiked with 10 μl of [^{3}H]cetyl alcohol was passed down the GPC column, and the presence of radioactivity detected by LSC. The entrapment efficiency (E) was calculated based on the ratio of radioactivity eluted in the void volume (P_1) and total radioactivity put on the column (P_t) from the relationship:

$$P_1/P_t = E \quad (1)$$

The radiolabeled compound release profile was assessed by a dialysis method. A volume of 300 μl of radiolabeled nanoparticle suspension was pipeted into DispoDialyzers (MWCO 100 kDa) and dialyzed against 20 ml of 10 mM PBS for 24 h at 4°C followed by up to 6 h at 37°C. At predetermined time points, 100 μl of sample was withdrawn, and radioactivity was measured by LSC.

Brain Uptake Studies

The uptake of [^{3}H]NPs into the brain was assessed using the *in situ* rat brain perfusion technique of Takasato *et al* (21) with modifications (22,23). Perfusions of 15–60 s were used to determine initial brain uptake of the nanoparticle formulations. All studies were approved by Texas Tech University HSC Institutional Animal Care and Use Committee and were conducted in accordance with the NIH Guide for the Care and Use of Laboratory Animals. For brain uptake studies, the radiolabeled nanoparticles were prepared on the day preceding the animal experiment. Vials were sealed and shipped at 4°C to Texas Tech University (Amarillo, TX), where transport experiments were performed.

In Situ Rat Brain Perfusion

Male Fischer-344 rats (220–330 g; Charles River Laboratories, Kingston, NY) were anesthetized with sodium pentobarbital (50 mg/kg intraperitoneal). A PE-60 catheter filled with heparinized saline (100 U/ml) was placed into the left common carotid artery after ligation of the left external carotid, occipital, and common carotid arteries. Common carotid artery ligation was accomplished caudal to the catheter implantation site. The pterygopalatine artery was left open during the experiments (22). Rat rectal temperature was monitored and maintained at 37°C by a heating pad con-

nected to a feedback device (YSI Indicating Controller, Yellow Springs, OH). The catheter to the left common carotid artery was connected to a syringe containing buffered physiologic perfusion fluid [containing (in mM): NaCl 128, $NaPO_3$ 2.4, $NaHCO_3$ 29.0, KCl 4.2, $CaCl_2$ 1.5, $MgCl_2$ 0.9, and D-glucose 9) with 1 μCi/ml [^{3}H]NP (final nanoparticle concentration ~20 μg/ml) and 0.3 μCi/ml [^{14}C]sucrose (to determine vascular volume). Perfusion fluid was filtered and warmed to 37°C and gassed with 95% O_2 and 5% CO_2. The pH and osmolarity of this solution were ~7.35 and 290 mOsm, respectively, immediately before perfusion. The perfusion fluid was infused into the left carotid artery with an infusion pump for periods of 15–60 s at 10 ml/min (Harvard Apparatus, South Natick, MA). This perfusion rate was selected to maintain a carotid artery pressure of ~120 mmHg (21).

Rats were decapitated, and cerebral samples obtained as previously described (24). Briefly, the brain was removed from the skull, and the perfused cerebral hemisphere dissected on ice after removal of the arachnoid membrane and meningeal vessels. Brain regions were placed in scintillation vials and weighed. In addition, two 50-μl aliquots of the perfusion fluid were transferred to a scintillation vial and weighed. The brain and perfusion fluid samples were then digested overnight at 50°C in 1 ml of 1 M piperidine. Ten milliliters of Fisher Chemical scintillation cocktail (Beckman, Fullerton, CA) was added to each vial, and the tracer contents assessed by dual-label liquid scintillation counting. Dual-labeled scintillation counting of brain and perfusate samples were accomplished with correction for quench, background, and efficiency.

Kinetic Analysis

Concentrations of nanoparticle tracer in brain and perfusion fluid are expressed as dpm/g brain or dpm/ml perfusion fluid, respectively. Blood–brain barrier [^{3}H]NP transport into the brain was determined by perfusion with [^{3}H]NP in separate experiments for 15- to 60-s periods as described previously (21,23). Unidirectional uptake transfer constants (K_{in}) were calculated from the following relationship to the linear portion of the uptake curve as described (23) from the equation:

$$Q^*/C^* = K_{in}T + V_o \quad (2)$$

where Q* is the quantity of [^{3}H]tracer in brain (dpm/g) at the end of perfusion, C* is the perfusion fluid concentration of [^{3}H]NP (dpm/ml), T is the perfusion time (s), and V_o is the extrapolated intercept (T = 0 s; "vascular volume" in ml/g). Tracer trapped in the vascular space was accounted for by the subtraction of [^{14}C]sucrose vascular volume.

Cerebral perfusion flow rate (F) was determined in separate experiments in the presence both NP formulations (25). C_{pf} is the perfusion fluid concentration of tracer [^{3}H]NP, and T is the net perfusion time. K_{in} values were then converted to apparent cerebrovascular permeability–surface area products (PA) using the Crone-Renkin equation (23),

$$PA = -F \ln(1 - K_{in}/F) \quad (3)$$

Statistical Analyses

Data presented are from the frontal cerebral cortex unless otherwise specified. [^{3}H]NP brain uptake and PA reduction over time were fit with nonlinear regression using least-squares analysis. For all data, errors are reported as the standard error of the mean unless otherwise indicated (GraphPad Prism Version 3.00 for Windows, GraphPad Software, San Diego, CA).

RESULTS

Our laboratory has recently reported on a novel method to engineer nanoparticles from microemulsion precursors (20,26,27). Two of the most promising systems, E. Wax and Brij 72, were chosen for further testing as brain drug delivery systems. The novel nanoparticles are composed of biocompatible materials: emulsifying wax and Brij 72 as the nanoparticle matrix materials, and Brij 78 and Tween 80 as surfactants. Both nanoparticle formulations have particle sizes below 100 nm (20). One of the major requirements for effective nanoparticle brain delivery is small size; thus, *in vitro* stability of nanoparticles in aqueous suspension was tested over a period of 1 week at room temperature, –20°C (data not shown), and 4°C. Both nanoparticle preparations showed superior stability at 4°C as compared to 25°C or –20°C. The initial size of E72 NPs stored at 4°C increased by 50% and 88% on day 2 and 4, respectively (Table I). By the end of 1 week, the nanoparticles had increased in mean size by 100%. E78 NPs were generally more stable than the E72 NPs. When stored at 4°C, E78 NPs increased in mean size by about 60% over the period of 1 week. The tendency of the nanoparticles to increase in size during storage is not fully understood. It is possible that because of the high surface area of nanoparticles in suspension, larger particles grow at the expense of the smaller ones in order to reduce the overall free energy of the system (i.e., Ostwald ripening). Table II shows the stability of both E78 NP and E72 NP formulations in various biologically relevant media at 37°C. Particle size analysis revealed no significant changes in particle size at physiologic temperature, suggesting that both nanoparticle systems remained intact during the time course of *in situ* perfusion experiments. These stability data agree with previous findings (20).

In order to ascertain nanoparticle brain uptake, both formulations were radiolabeled with [^{3}H]cetyl alcohol. Hydrogen substitution by tritium [^{3}H] atom was made on the first carbon to avoid the possibility of ^{3}H hydrogen exchange with water during the time of experiments. The choice of radioactive compound was based on the fact that E. wax is composed

Table I. Short-Term Stability of Nanoparticles at 4°C

	Nanoparticle size (nm)	
Time (days)	NP E78	NP E72
0	58 ± 0.8	98 ± 1.8
2	78 ± 1.4	147 ± 0.8
4	87 ± 0.5	184 ± 4.1
7	95 ± 1.1	206 ± 6.8

E. wax nanoparticles (E78 NP) and Brij 72 nanoparticles (E72 NP) were prepared from warm microemulsion precursors. Particle sizes were measured immediately after preparation (day 0). Both types of preparations were sealed and stored at 4°C for a period of 1 week. Before nanoparticle size measurement, aliquots of samples were allowed to equilibrate to room temperature. Data presented are mean ± SEM (n = 3).

Table II. Stability of Nanoparticles in Various Biologically Relevant Media at 37°C

	Nanoparticle size (nm)			
	NP E72		NP E78	
Medium	Initial time	1 h	Initial time	1 h
Water	52.8 ± 3.9	54.3 ± 7.3	81.5 ± 9.1	77.5 ± 4.3
10 mM PBS	55.1 ± 5.3	57.0 ± 5.5	73.0 ± 9.4	81.6 ± 9.2
150 mM NaCl	57.8 ± 5.7	57.7 ± 5.7	72.8 ± 9.1	83.7 ± 8.9
10% FBS	35.4 ± 4.3	40.7 ± 6.5	52.9 ± 8.2	56.6 ± 4.9

E. Wax and Brij 72 nanoparticles were diluted (1:10 v/v) with water, 10 mM phosphate-buffered saline (PBS), 150 mM sodium chloride (NaCl), or 10% (v/v) fetal bovine serum in 150 mM NaCl (FBS). Particle sizes were measured immediately after dilution and after 1 h of incubation at 37°C. Data reported are mean ± SEM (n = 3).

of a mixture of cetostearyl alcohol and polysorbate 60 (4:1 w/w) (28). It was hypothesized that trace amounts of [^{3}H]cetyl alcohol would be easily entrapped in E78 NPs, and minimal or no release would be seen. Hexadecanol is practically insoluble in water. Thus, during the radiolabeling procedure, care was taken to remove all solvent in which cetyl alcohol was supplied. It was also confirmed that the labeling procedure did not affect the size of solid nanoparticles (data not shown). The entrapment efficiency of [^{3}H]cetyl alcohol was determined by comparing the activity of [^{3}H]NPs before and after separation on a gel permeation chromatography column. For both nanosuspension types, all radioactivity coeluted with nanoparticles in the void volume, indicating high entrapment efficiency (Fig. 1). These findings were also confirmed by lack of appearance of a second peak caused by elution of free [^{3}H]cetyl alcohol. To ensure stability of [^{3}H]NPs and association of the label with nanoparticles under conditions in which formulations were ultimately exposed, nanosuspensions were dialyzed against 10 mM phosphate-buffered saline (pH 7.4) for 24 h at 4°C and 6 h at 37°C (Fig. 2). For E72 NPs, about 2% of the total radioactivity was released after initial dialysis at 4°C. The amount of free radiolabel remained constant throughout the course of experiment. In the case of E. Wax nanoparticles, a constant level of about 2% radioactivity was detected in dialysis buffer after 24 h at 4°C, and up to 30 min at 37°C. After that time, a slight increase of release was noted, but it reached only 4% after 6 h at 37°C. Of concern was whether released radioactivity could be related to trace amounts of [^{3}H]water and/or [^{3}H]methanol. The presence of these compounds could create some error during brain uptake measurements. It was shown that the steady release of radioactivity from nanoparticles occurs within first 90 min, after which it reaches a plateau. Additionally, released material passed down the GPC column eluted in the same fraction as the free unentrapped [^{3}H]cetyl alcohol standard. It was thus concluded that the radioactivity detected in the release buffer represented unentrapped [^{3}H]cetyl alcohol probably remaining on the surface of the nanoparticles.

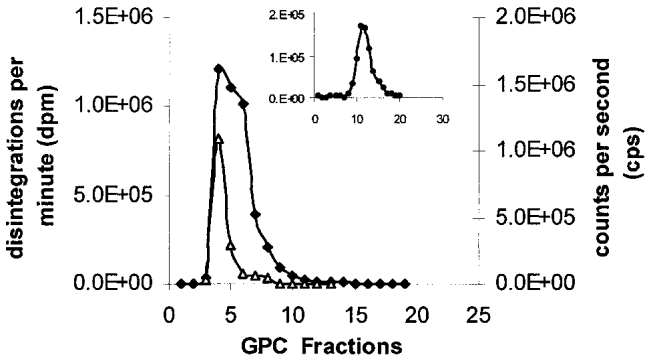

Fig. 1. Entrapment efficiency of [^{3}H]cetyl alcohol in E72 nanoparticles using gel permeation chromatography (GPC) elution profiles. The GPC fractions containing cold nanoparticles were detected by laser light scattering (counts per second). [^{3}H]NP and [^{3}H]cetyl alcohol were counted by a liquid scintillation counter and expressed as disintegrations per minute (dpm): (Δ) counts per second (cps) for cold E72 nanoparticles, (♦) dpm for [^{3}H]E72 NP. The insert shows the profile for [^{3}H]cetyl alcohol alone (•).

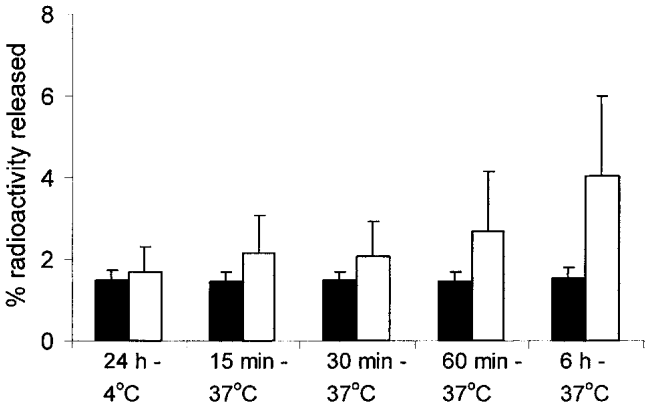

Fig. 2. Release profile of [^{3}H]cetyl alcohol from E78 nanoparticles (*white bars*) and E72 nanoparticles (*black bars*). Both preparations were dialyzed against 10 mM phosphate-buffered saline at 4°C for 24 h and then at 37°C up to 6 h. (n = 3 for each preparation)

Brain distribution parameters of [^{3}H]NPs were evaluated using the *in situ* rat brain perfusion method. Uptake of [^{3}H]NPs (1 μCi/20 μg/ml) into the brain was evaluated from 0 to 60 s. Brain/perfusion fluid ratios (i.e., volume of distribution or "space") were plotted as a function of time and are illustrated in Fig. 3. The integrity of the BBB was verified during each experiment by simultaneous vascular volume measurements using [^{14}C]sucrose. [^{14}C]Sucrose vascular volumes in this study ranged from 0.8 ± 0.2 to 1.2 ± 0.2 × 10^{-2} ml/g consistent with an intact BBB during the experimental time frame and previous *in situ* nanoparticle perfusion data (25).

BBB transfer coefficient values (K_{in}) were calculated from the slope of the [^{3}H]NP brain accumulation vs. time graph [Eq. (2)] (23). Brain accumulation is defined as the brain/perfusate concentration ratio vs. time and is represented in Fig. 3. The calculated K_{in} and PA for [^{3}H]NP E72 were 5.7 ± 1.1 × 10^{-3} ml/s/g and 6.1 ± 1.4 × 10^{-3} ml/s/g, respectively (r^2 = 0.922) (Fig. 3). A significant difference between [^{14}C]sucrose and [^{3}H]E72 NPs transfer coefficients was observed ($p < 0.001$), suggesting brain nanoparticle distribution. The calculated K_{in} and PA for the [^{3}H]E78 NPs as shown in Fig. 3 were 4.1 ± 0.5 × 10^{-3} ml/s/g and 4.3 ± 0.7 × 10^{-3} ml/s/g, respectively (r^2 = 0.973). Similar to [^{3}H]E72 NP data, a significant difference between the [^{14}C]sucrose and nanoparticle formulation transfer coefficients was observed ($p < 0.001$).

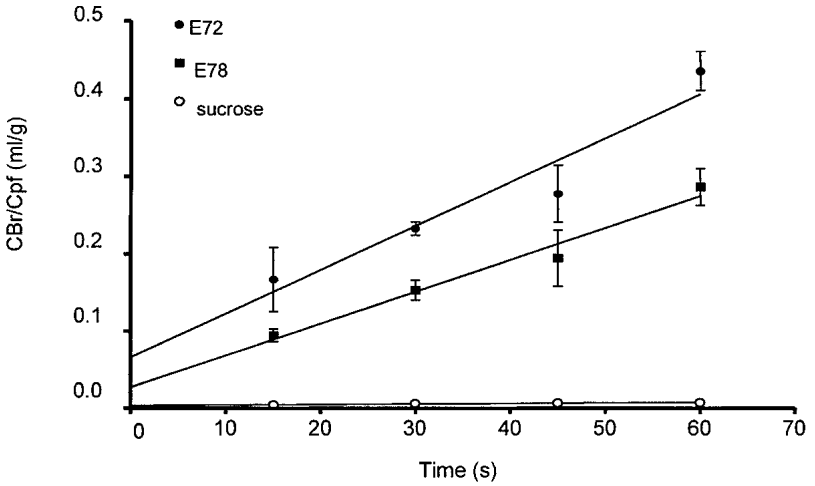

Fig. 3. Time course of [^{3}H]NPs and [^{14}C]sucrose uptake into rat brain during perfusion times of 15 to 60 s. The unidirectional transfer coefficient (K_{in}) was calculated from the slope of the [^{3}H]NP brain accumulation vs. time curve [Eq. (1)]. K_{in} values were 5.67 $\pm$ 1.1 $\times$ 10^{-3} ml/s/g and 4.11 $\pm$ 0.5 $\times$ 10^{-3} ml/s/g for E72 NP and E78 NP, respectively. A significant difference was noted between [^{3}H]NP and [^{14}C]sucrose distribution parameters ($p < 0.001$) and between both nanoparticle types ($p < 0.05$).

DISCUSSION

The data presented herein suggest that both nanoparticle formulations could be transported across the BBB; however, the mechanism of transport has not been elucidated. Kreuter and Alyautdin (29) argued that the transport of poly(butylcyanoacrylate) nanoparticles containing drug in their experiments could be related to a number of different mechanisms, such as (a) formation of a drug concentration gradient as a result of nanoparticle adhesion to endothelium and subsequent drug release, (b) blocking of pgp by the surfactant Tween 80 resulting in subsequent higher brain uptake of drug, (c) toxic effects of the nanoparticle components on the BBB, (d) opening of the endothelium barrier by the presence of surface active agents such as Tween 80, and/or (e) endocytosis and/or transcytosis of nanoparticles by endothelial cells.

In the present study, the uptake of drug-free radiolabeled nanoparticles was investigated, thereby most likely eliminating mechanisms (a) and (b). To evaluate effects of E. Wax and Brij 72 NPs on the blood–brain barrier, the baseline BBB parameters were screened in the presence of both types of nanoparticle (25). The *in situ* rat brain perfusion method was used to investigate the influence of E78 NPs and E72 NPs on cerebral perfusion flow, barrier integrity, and permeability. Similar studies were performed *in vitro* using bovine brain microvessel endothelial cells, an established *in vitro* BBB model. The effects of nanoparticles on bovine brain microvessel endothelial cells were tested, evaluating barrier integrity, permeability, choline transport, and tight junctional protein expression. *In vivo* and *in vitro* studies revealed no statistically significant changes in BBB integrity, permeability, or facilitated choline transport. The presence of either nanoparticle did not lead to any significant differences in cerebral perfusion flow *in vivo*. Additionally Western blot analysis confirmed that the incubation of nanoparticles with bovine brain microvessel endothelial cells did not alter occludin and claudin-1 expression. It was concluded that E78 and E72 NPs have minimal effect on baseline BBB parameters; therefore, the brain uptake values observed in the present study are not likely to be caused by toxic effects of nanoparticles on the BBB. Furthermore, mechanisms (c) and (d) seem unlikely in the present studies because [^{14}C]sucrose brain distribution "space" did not increase in the presence of the nanoparticles evaluated.

It is well known that surface-active agents can compromise membrane integrity and increase permeability to drugs and other molecules. In fact, in the case of poly(butylcyanoacrylate) nanoparticles reported by Kreuter *et al.*, only Tween 80–coated nanoparticles were successful in delivering drugs across the BBB. Further, no pharmacologic effects were observed with uncoated nanoparticles. In these present studies, E72 NPs that contained Tween 80 resulted in a statistically significant increase in brain transport over E78 NPs ($p < 0.05$). This is in general agreement with Kreuter's reports (10,19,29). If the surfactant effect on the BBB was nonspecific, it could be argued that the presence of any surfactant should have similar effect on the BBB. However, it was reported that differences in brain uptake were seen when poly(methylmethacrylate) nanoparticles were coated with various different surfactants (18). Additionally, the Tween 80 used in the E72 NPs is hypothesized to have different physical characteristics than the same surfactant on the surface of poly(butylcyanoacrylate) nanoparticles. In previous reports, the Tween 80 was allowed to adsorb on the surface of preformed PBCA nanoparticles. In contrast, in the case of E72 NPs, Tween 80 was added to form the microemulsion precursors, which were subsequently used to form solid nanoparticles. Thus, it is thought that the hydrophobic tail of Tween 80 was located in the warm oil droplet and the hydrophilic head group was extended into the external aqueous environment. Upon cooling of the microemulsion precursor and during solid nanoparticle formation, the surfactant was thought to be immobilized within nanoparticles with only the hydrophilic head group being exposed on the surface. This immobilization of the surfactant in the nanoparticles would likely minimize, if not eliminate, the surface-active properties of the surfactant. Al-

though this hypothesis was not directly proven in these present studies, previous reports of coating the nanoparticles with hydrophobically modified folate ligands confirmed this phenomenon (30,31). The E72 NPs contain only 2.3 mM Tween 80, whereas a threefold higher concentration was postcoated on the surface of the reported PBCA nanoparticles. Thus, although Tween 80 may be a factor altering BBB permeability in presence of PBCA nanoparticles, it does not influence the BBB integrity in the case of E78 and E72 NP exposure (25). BBB integrity was confirmed in the present study to be maintained as well. Initial washout studies have been performed and indicate absence of [^{3}H]NPs loosely associated with endothelium (data not shown).

Based on this study and arguments presented above, it could be suggested that endocytosis and/or transcytosis is a plausible explanation for the presented results. Additionally, brain uptake was measured over short time during which significant uptake was observed. Therefore, it is possible that passive permeability of the nanoparticles may also have a role in transport across BBB. At this time no argument confirming or contradicting endocytotic uptake and/or passive diffusion is evident. Additional experiments are under way to elucidate the mechanism of transport. Washout experiments will be continued, and capillary depletion studies will follow to quantify nanoparticles trapped in the cells and determine whether E72 and/or E78 NPs are found in the brain tissue or are trapped in the brain vascular endothelium.

CONCLUSIONS

Two different types of nanoparticles were engineered directly from warm microemulsion precursors. Both nanoparticle types were radiolabeled by entrapment of [^{3}H]cetyl alcohol, and their brain uptake evaluated *in situ* using the rat brain perfusion method. BBB transfer coefficients from perfusion fluid to the brain were $5.7 \pm 1.1 \times 10^{-3}$ ml/s/g and $4.1 \pm 0.5 \times 10^{-3}$ ml/s/g for E72 NPs and E78 NPs, respectively. Significant brain uptake compared to [^{14}C]sucrose suggests transport across the BBB. The mechanism of transport has not been elucidated. More experiments are planned to fully understand the BBB permeability to these nanoparticle formulations.

ACKNOWLEDGMENTS

The research was supported, in part, by NIH/NIBIB grant EB00531-01. The authors would also want to gratefully acknowledge the School of Pharmacy and the Vascular Biology Research Center at Texas Tech University Health Sciences Center, the American Federation for Aging Research: Glen AFAR Research Scholarship Project and an American Foundation for Pharmaceutical Education predoctoral fellowship for financial support.

REFERENCES

1. W. M. Pardridge. *Brain Drug Targeting, The Future of Brain Drug Development*, Cambridge University Press, Cambridge, UK, 2001.
2. A. Tsuji. Specific mechanisms for transporting drugs into brain. In D. J. Begley, M.W. Bradbury, J. Kreuter (eds.), *The Blood-Brain Barrier and Drug Delivery to the CNS*, Marcel Dekker, New York, 2000, pp. 121–144.
3. C. Krewson and W. M. Saltzman. Transport and elimination of recombinant human NGF during long-term delivery to the brain. *Brain Res.* **727**:169–181 (1996).
4. C. Krewson, M. L. Klarman, and W. M. Saltzman. Distribution of nerve growth factor following direct delivery to brain interstitium. *Brain Res.* **680**:196–206 (1995).
5. L. Illum. Transport of drugs from the nasal cavity to the central nervous system. *Eur. J. Pharm. Sci.* **11**:1–18 (2000).
6. S. Mathison, R. Nagilla, and U. B. Kompella. Nasal route for direct delivery of solutes to the central nervous system: fact or fiction? *J.Drug. Targ.* **5**:415–441 (1998).
7. A. Granholm, D. Albeck, C. Backman, M. Curtis, T. Ebendal, P. Frieden, M. Henry, B. Hoffer, J. Kordower, G. M. Rose, S. Soderstrom, and R. T. Bartus. A non-invasive system for delivering neural growth factors across the blood-brain barrier: a review. *Rev. Neurosci.* **9**:31–55 (1998).
8. P. R. Lockman, R. J. Mumper, M. A. Khan, and D. D. Allen. Nanoparticle technology for drug delivery across the blood-brain barrier. *Drug Dev. Ind. Pharm.* **28**:1–12 (2002).
9. K. S. Soppimath, T. M. Aminabhavi, A. R. Kulkarni, and W. E. Rudzinski. Biodegradable polymeric nanoparticles as drug delivery devices. *J. Control. Rel.* **70**:1–20 (2001).
10. J. Kreuter. Nanoparticulate systems for brain delivery of drugs. *Adv. Drug Del. Rev* **47**:65–81 (2001).
11. R. N. Alyautidin, E. B. Tezikov, P. Ramage, D. A. Kharkevich, D. J. Begly, and J. Kreuter. Significant entry of tubocurarine into the brain of rats by adsorption to polysorbate 80-coated poly(butylcyanoacrylate) nanoparticles: an *in situ* brain perfusion study. *J. Microencap.* **15**:67–74 (1998).
12. U. Schroder and B. A. Sabel. Nanoparticles, a drug carrier system to pass the blood-brain barrier, permit central analgesic effects of i.v. dalargin injections. *Brain Res.* **710**:121–124 (1996).
13. A. Gulyaev, S. E. Gelperina, I. N. Skidan, A. S. Antropov, G. Y. Kivman, J. Kreuter. Significant transport of doxorubicin into the brain with polysorbate 80 coated nanoparticles. *Pharm. Res.* **16**: 1564–1569 (1999).
14. U. Schroder, P. Sommerfield, S. Urlich, and B. Sabel. Nanoparticle technology for delivery of drugs across the blood-brain barrier. *J. Pharm. Sci.* **78**:1305–1307 (1998).
15. R. N. Alyautidin, V. E. Petrov, K. Langer, A. Berthold, D. A. Kharkievich, and J. Kreuter. Delivery of loperamide across the blood-brain barrier with polysorbate 80-coated nanoparticles. *Pharm. Res.* **14**:325–328 (1997).
16. R. Alyautdin, D. Gothier, V. Petrov, D. Kharkevich, and J. Kreuter. Analgesic activity of the hexapeptide dalargin adsorbed on the surface of polysorbate 80-coated poly(butylcyanoacrylate) nanoparticles. *Eur. J. Pharm. Biopharm.* **41**:44–48 (1995).
17. S. C. Yang, L. F. Lu, Y. Cai, J. B. Zhu, B. W. Liang, and C. Z. Yang. Body distribution in mice of intravenously injected camptothecin solid lipid nanoparticles and targeting effect on brain. *J. Control. Release* **59**:299–307 (1999).
18. S. D. Troster, U. Muller, and J. Kreuter. Modification of the body distribution of poly(methylmethacrylate) nanoparticles in rats by coating with surfactants. *Int. J. Pharm.* **61**:85–100 (1990).
19. J. Kreuter, R. N. Alyautdin, D. A. Kharkevich, and A. A. Ivanov. Passage of peptides through the blood-brain barrier with colloidal polymer particles (nanoparticles). *Brain Res.* **674**:171–174 (1995).
20. M. O. Oyewumi and R. J. Mumper. Gadolinium loaded nanoparticles engineered from microemulsion templates. *Drug Dev. Ind. Pharm.* **28**:317–328 (2002).
21. Y. Takasato, S. I. Rapoport, and Q. R. Smith. An *in situ* brain perfusion technique to study cerebrovascular transport in the rat. *Am. J. Physiol.* **247**:484–493 (1984).
22. D. D. Allen, J. Oki, and Q. R. Smith. An update in the *in situ* rat brain perfusion technique: simpler, faster, better. *Pharm. Res.* **14** (suppl):337 (1997).
23. Q. R. Smith. Brain perfusion systems for studies of drug uptake and metabolism in the central nervous system. *Pharm. Biotechnol.* **8**:285–307 (1996).
24. D. D. Allen and Q. R. Smith. Characterization of the blood-brain barrier choline transporter using the *in situ* rat brain perfusion technique. *J. Neurochem.* **76**:1–11 (2001).

25. P. R. Lockman, J. Koziara, K. E. Roder, J. Paulson, T. J. Abbruscato, R. J. Mumper, and D. D. Allen. *In vivo* and *in vitro* assessment of baseline blood-brain barrier parameters in the presence of novel nanoparticles. *Pharm. Res.* **20**:705–713 (2003).
26. M. O. Oyewumi and R. J. Mumper. Engineering tumor-targeted gadolinium hexanedione nanoparticles for potential application in neutron capture therapy. *Bioconjugate Chem* **13**:1328–1335 (2002).
27. Z. Cui and R. J. Mumper. Plasmid DNA-entrapped nanoparticles engineered from microemulsion precursors: *in vitro* and *in vivo* evaluation. *Bioconjugate Chem.* **13**:1319–1327 (2002).
28. A. Wade. P. J Weller. *Handbook of Pharmaceutical Excipients*, American Pharmaceutical Association, Washington, 1994.
29. J. Kreuter and R. N. Alyautdin. Using nanoparticles to target drugs to the central nervous system. In D. J. Begley, M. W. Bradbury, and J. Kreuter (eds.), *The Blood-Brain Barrier And Drug Delivery To The CNS*, Marcel Dekker, New York, 2000, pp. 205-223.
30. M. O. Oyewumi and R. J. Mumper. Engineering tumor-targeted gadolinium hexanedione nanoparticles for potential application in neutron capture therapy. *Bioconjugate Chem.* **13**:1328–1335 (2002).
31. M. O. Oyewumi and R. J. Mumper. Influence of formulation parameters on gadolinium entrapment and tumor cell uptake using folate-coated nanoparticles. *Inter. J. Pharm.* **251**:85–97 (2003).